

Histogram Matching Augmentation for Domain Adaptation with Application to Multi-Centre, Multi-Vendor and Multi-Disease Cardiac Image Segmentation

Jun Ma^[0000-0002-9739-0855]

Department of Mathematics, Nanjing University of Science and Technology
junma@njjust.edu.cn

Abstract. Convolutional Neural Networks (CNNs) have achieved high accuracy for cardiac structure segmentation if training cases and testing cases are from the same distribution. However, the performance would be degraded if the testing cases are from a distinct domain (e.g., new MRI scanners, clinical centers). In this paper, we propose a histogram matching (HM) data augmentation method to eliminate the domain gap. Specifically, our method generates new training cases by using HM to transfer the intensity distribution of testing cases to existing training cases. The proposed method is quite simple and can be used in a plug-and-play way in many segmentation tasks. The method is evaluated on MICCAI 2020 M&Ms challenge, and achieves average Dice scores of 0.9051, 0.8405, and 0.8749, and Hausdorff Distances of 9.996, 12.49, and 12.68 for the left ventricular, myocardium, and right ventricular, respectively. Our results rank the third place in MICCAI 2020 M&Ms challenge. The code and trained models are publicly available at https://github.com/JunMa11/HM_DataAug.

Keywords: Cardiac Segmentation · Deep learning · Domain adaptation · Histogram Matching · Generalization

1 Introduction

Accurate segmentation of the left ventricular cavity, myocardium and right ventricle from cardiac magnetic resonance images plays an import role for quantitative analysis of cardiac function, which can be used in clinical cardiology for patient management, disease diagnosis, risk evaluation, and therapy decision [11]. In the recent years, many deep learning-based methods have achieved unprecedented performance ([1] [3]), especially when testing cases have the same distribution as training cases. However, segmentation accuracy can be greatly degraded when these methods are tested on unseen datasets acquired from distinct MRI scanners or clinical centres [12]. This problem makes it difficult for these methods to be applied consistently across multiple clinical centres, especially when subjects are scanned using different MRI protocols or machines.

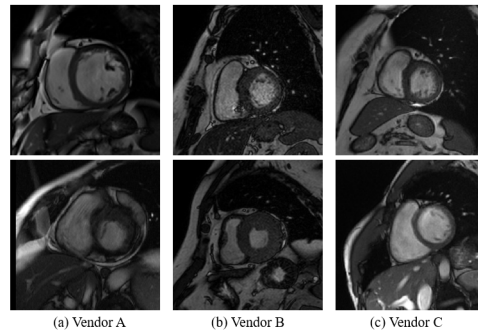


Fig. 1. Visual examples from different vendors. Images from different vendors have significant appearance variations.

The M&Ms challenge is the first international competition to date on cardiac image segmentation combining data from different centres, vendors, diseases and countries at the same time. It evaluates the generalisation ability of machine/deep learning and cross-domain transfer learning techniques for cardiac image segmentation [2]. Figure 1 shows six cardiac MR cases from three vendors. It can be observed that the appearance varies remarkably among different vendors. Thus, how to develop a robust segmentation model that it can generalize to different centers, vendors, and diseases is an important but challenging problem.

Recently, many studies have been proposed to tackle this issue, such as domain adaptation ([6], [4]) and domain generalization [5]. Basically, domain adaptation aims to learn to align source and target domain in a domain-invariant high level feature space, which usually needs few annotated or unlabelled cases from the target domain during training. Domain generalization aims to train a model that it can directly generalize to new domains without need of retraining, which does not use data from the target domain. In practice, both the two popular methods need to modify network architectures or loss functions.

Motivated by a recent study [7] where CNNs are more sensitive to texture and intensity features. We aim to improve the generalization ability of CNNs by transferring the intensity distribution of the target dataset to the source dataset. Specifically, we use histogram matching to bring the intensity appearance of the target dataset to the source dataset. Instead of modifying the network architecture or loss function, our method only augments the training dataset, which is very simple and can be a plug-and-play method to any segmentation tasks.

2 Proposed Method

Histogram matching has been a widely used method, which generates a processed image with a specified histogram [8]. We give a formal introduction of histogram matching as follows. Let S and T denote continuous intensities (considered as random variables) of the source image and the target image, respectively. P_S and

P_T denote their corresponding continuous probability density functions (PDF). We can estimate P_S from the source image, and P_T is the target probability density function. Let r be a random variable with the property

$$r = M(S) = (L - 1) \int_0^S P_S(x) dx, \quad (1)$$

where L is the number of intensity levels and x is a dummy variable of integration. Suppose that a random variable w has the property

$$G(T) = (L - 1) \int_0^T P_T(x) dx = r, \quad (2)$$

it then follows from these two equations that $M(S) = G(T)$ and therefore, that T must satisfy the condition

$$T = G^{-1}[M(S)] = G^{-1}(r) \quad (3)$$

Equations (1)-(3) show that an image whose intensity levels have a specified probability density function can be obtained from a given image by using the following four steps:

- Step 1. Obtain P_S from the source image and use Eq. (1) to obtain the value of r .
- Step 2. Use the specified PDF in Eq. (2) to obtain the transformation function $G(T)$.
- Step 3. Obtain the inverse transformation $T = G^{-1}(r)$.
- Step 4. Obtain the output image by first equalizing the input image using Eq. (1); the pixel values in this image are the r values. For each pixel with value r in the equalized images, perform the inverse mapping $T = G^{-1}(r)$ to obtain the corresponding pixel in the output image. When all pixels have been thus processed, the PDF of the output image will be equal to the specified PDF.

Scikit-image [13] has a build-in function `match_histograms`¹ for histogram matching. In this paper, we use histogram matching to augment the training dataset so as to introduce the intensity distribution of the testing set. Specifically, we randomly select image pairs from labelled cases and unlabelled cases, and then transform the intensity distribution of the unlabelled case to labelled case. In this way, we can obtain many new training cases where its intensity distribution is similar to the unlabelled cases. Figure 2 presents some examples of the source images, target images and augmented images.

3 Experiments and Results

3.1 Dataset and training protocols

Dataset The M&Ms challenge cohort is composed of 350 patients with hypertrophic and dilated cardiomyopathies as well as healthy subjects. All subjects

¹ <https://scikit-image.org/docs/stable/>

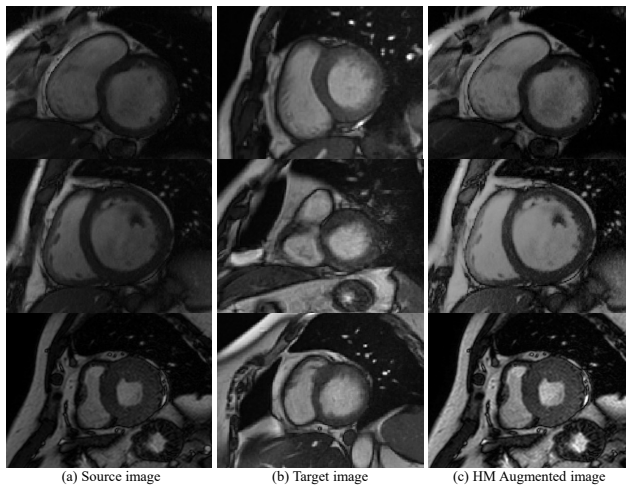


Fig. 2. Visual examples of the augmented images by histogram matching.

were scanned in clinical centres in three different countries (Spain, Germany and Canada) using four different magnetic resonance scanner vendors (Siemens, General Electric, Philips and Canon). The training set will contain 150 annotated images from two different MRI vendors (75 each) and 25 unlabelled images from a third vendor. The CMR images have been segmented by experienced clinicians from the respective institutions, including contours for the left (LV) and right ventricle (RV) blood pools, as well as for the left ventricular myocardium (MYO). The 200 test cases correspond to 50 new studies from each of the vendors provided in the training set and 50 additional studies from a fourth unseen vendor, that will be tested for model generalization ability. 20% of these datasets will be used for validation and the rest will be reserved for testing and ranking participants.

During preprocessing, we resample all the images to $1.25 \times 1.25 \times 8mm^3$ and apply Z-score (mean subtraction and division by standard deviation) to normalize each image. We employ nnU-Net [9] as the default network. The patch size is $288 \times 288 \times 14$, and batch size is 8. We train 2D U-Net and 3D U-Net with five-fold cross validation. Each fold is trained on a TITAN V100 GPU with 1000 epochs. For each fold, we save the best-epoch model² and final-epoch model. The code and trained models will be publicly available for research community after anonymous review. We declare that the segmentation method has not used any pre-trained models nor additional MRI datasets other than those provided by the organizers.

² Best-epoch model stands for the model that can achieves the best Dice on the validation set.

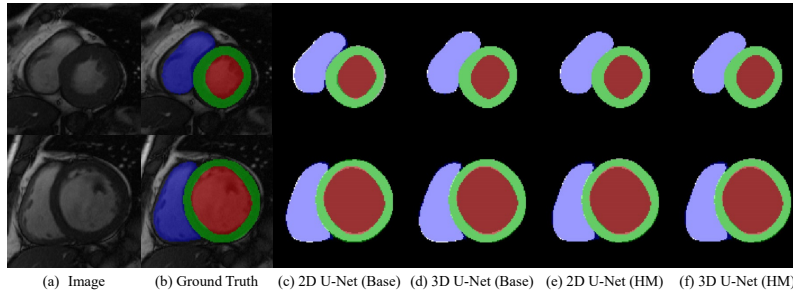


Fig. 3. Visual examples of segmentation results. Base and HM stand for the baseline dataset and the histogram matching augmented dataset.

3.2 Five-fold cross validation results

Table 1 presents the five-fold cross validation results of the final-epoch models of 2D U-Net and 3D U-Net³. Basically, we found that the performance of 3D U-Net is slightly better than 2D U-Net. Figure 3 presents some visual segmentation results of different models. The methods achieve the best Dice scores for left ventricular, while the performance of myocardium is inferior than the left and right ventricular, indicating that the myocardium is more challenging to obtain accurate segmentation results.

3.3 Validation set results

The validation set is hidden by challenge organizers. We package our code and model in a singularity container and submit it to the organizers. Due to the limited number of submission tries, we do not submit the baseline models because the models trained on augmented datasets would be better than baseline models. In summary, we submit the following five solutions on the validation set.

- Solution 1. 3D U-Net best-epoch model;
- Solution 2. 3D U-Net final-epoch model;
- Solution 3. Ensemble of 3D U-Net best-epoch model and 2D U-Net best-epoch model;
- Solution 4. Ensemble of 3D U-Net final-epoch model and 2D U-Net final-epoch model;
- Solution 5. Ensemble of the above four solutions;

Table 2 shows the quantitative results of the five solutions on validation set. It can be observed that assembling multiple models may improve Dice, but would degrade the HD and ASSD. We also apply paired T-test between the solution 1 and the other four solutions to show whether their performances are statistically

³ The results corresponding to the best-epoch model are not reported because it overfits the validation set, where the corresponding Dice score is meaningless.

Table 1. Five-fold cross validation results. It should be noted that The models trained on the default and the augmented dataset are not comparable, because the five-fold splits are different between the two datasets.

Dataset	Model	Fold	LV_Dice	Myo_Dice	RV_Dice
Default Dataset (Baseline)	2D U-Net	0	0.9124	0.8695	0.8842
		1	0.9254	0.8756	0.9074
		2	0.9218	0.8753	0.8945
		3	0.9265	0.8684	0.8845
		4	0.9291	0.8645	0.8874
	3D U-Net	0	0.9256	0.8873	0.8981
		1	0.9344	0.8879	0.9141
		2	0.9399	0.8828	0.9010
		3	0.9372	0.8760	0.8930
		4	0.9308	0.8753	0.8944
Histogram Matching Augmented Dataset	2D U-Net	0	0.9832	0.9639	0.9762
		1	0.9871	0.9729	0.9825
		2	0.9871	0.9747	0.9803
		3	0.9831	0.9683	0.9784
		4	0.9835	0.9735	0.9772
	3D U-Net	0	0.9895	0.9633	0.9760
		1	0.9887	0.9690	0.9826
		2	0.9824	0.9632	0.9719
		3	0.9871	0.9654	0.9796
		4	0.9870	0.9741	0.9762

significant different. Surprisingly, the statistical significance level $p > 0.05$ for all comparisons. In other words, the performances of solution 2-4 do not have statistically significant difference compared with the solution 1. It can be found that ensemble more models can obtain slightly better Dice scores, but could degrade the Hausdorff distance. We also compare our results with the recent work [10] that uses GAN for domain adaptation, and our methods obtain better Dice scores for LV, Myo and RV. Finally, we select the solution 1 as our final solution for the hidden testing set.

Table 2. Quantitative results of different solutions on the official hidden validation set. ‘-’ denotes not reported.

Solution	LV			Myo			RV		
	Dice	HD	ASSD	Dice	HD	ASSD	Dice	HD	ASSD
Solution 1	0.9130	8.089	1.017	0.8627	12.19	0.710	0.8937	11.88	0.9078
Solution 2	0.9131	8.091	1.015	0.8627	12.20	0.710	0.8935	11.85	0.9101
Solution 3	0.9166	8.090	0.958	0.8660	12.25	0.734	0.8927	11.35	0.9682
Solution 4	0.9166	8.103	0.959	0.8658	12.26	0.736	0.8927	11.34	0.9667
Solution 5	0.9166	8.099	0.959	0.8659	12.25	0.735	0.8927	11.35	0.9674
GAN [10]	0.903	-	-	0.859	-	-	0.865	-	-

3.4 Testing set results

Table 3 presents the average Dice, HD and ASSD for each vendor on testing set. Overall, the performances on vendor C and D are lower than the performances on vendor A and B, because the training set does not have annotated cases from the vendor C and D. It can be observed that the performance on the vendor C is better than the performance on the vendor D, especially in HD and ASSD with improvements up to $5mm$, which could⁴ demonstrate the effectiveness of our histogram matching data augmentation.

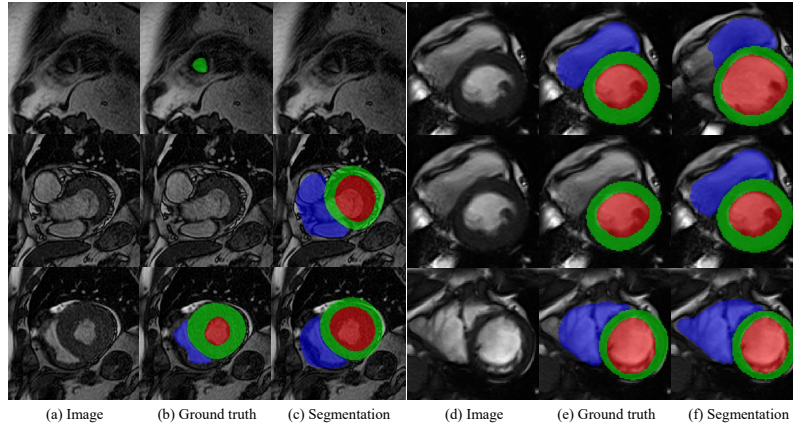


Fig. 4. Visual examples of worse cases in vendor A and B.

Table 3. Quantitative results on the official hidden testing set

Vendor	LV			Myo			RV		
	Dice	HD	ASSD	Dice	HD	ASSD	Dice	HD	ASSD
A	0.9148	10.78	1.003	0.8435	14.14	0.697	0.8771	12.84	1.142
B	0.9136	7.866	0.971	0.8675	10.14	0.717	0.8792	11.61	1.144
C	0.8943	9.231	1.389	0.8265	11.33	1.066	0.8732	10.82	1.152
D	0.8977	12.11	1.521	0.8243	14.34	0.958	0.8703	15.46	1.513
All	0.9051	9.996	1.221	0.8405	12.49	0.859	0.8749	12.68	1.238

Worse cases analysis Figure 4 and 5 show some segmentation results with low performance. Basically, it can be observed that most of the segmentation

⁴ Here we use ‘could’ because we do not have corresponding testing results of our baseline model where histogram matching data augmentation is not used.

errors occur in the top or bottom of the heart because these regions usually have low contrast and ambiguous boundaries. We find that the worse segmentation results can also have reasonable shapes even for the severe over-segmentation (e.g., Figure 4 the 2nd row). Some LV segmentation results are significantly smaller or larger than ground truth, which could motivate us to improve our network by imposing size constrain, such as constraining the volume of network outputs to be within a specified range.

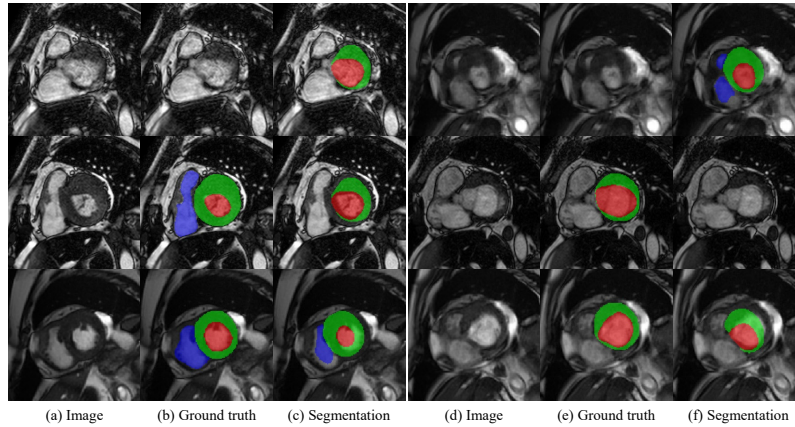


Fig. 5. Visual examples of worse cases in vendor C and D.

Limitation Although histogram matching is a good pre-processing technique to eliminate intensity distribution differences, it should be noted that histogram matching could cover specific characteristics of other MRI modalities, like for example, LGE MRI. With the histogram changes, relevant informations about scar tissue might be degraded. In the future, we need to verify the effects of histogram matching data augmentation on multi-sequence cardiac MR datasets, such as MyoPS [14].

4 Conclusion

One of the challenging problems of current segmentation CNNs is that the performance would degrade when applying the trained model to a new dataset. In this paper, we introduce histogram matching to augment the training cases that have the similar intensity distributions to the new (unlabelled) dataset set, which is very simple and can be a plug-and-play method to any segmentation CNNs. Based on the quantitative results on the validation set, we believe that our method can be a strong baseline.

Acknowledgement

The authors of this paper declare that the segmentation method they implemented for participation in the M&Ms challenge has not used any pre-trained models nor additional MRI datasets other than those provided by the organizers. We also thank the organizers for hosting the great challenge.

References

1. Bernard, O., Lalonde, A., Zotti, C., Cervenansky, F., Yang, X., Heng, P.A., Cetin, I., Lekadir, K., Camara, O., Ballester, M.A.G., et al.: Deep learning techniques for automatic mri cardiac multi-structures segmentation and diagnosis: is the problem solved? *IEEE Transactions on Medical Imaging* **37**(11), 2514–2525 (2018)
2. Campello, V.M., Palomares, J.F.R., Guala, A., Marakas, M., Friedrich, M., Lekadir, K.: Multi-Centre, Multi-Vendor & Multi-Disease Cardiac Image Segmentation Challenge (Mar 2020). <https://doi.org/10.5281/zenodo.3715890>
3. Chen, C., Qin, C., Qiu, H., Tarroni, G., Duan, J., Bai, W., Rueckert, D.: Deep learning for cardiac image segmentation: A review. *Frontiers in Cardiovascular Medicine* **7**, 25 (2020)
4. Chen, C., Dou, Q., Jin, Y., Chen, H., Qin, J., Heng, P.A.: Robust multimodal brain tumor segmentation via feature disentanglement and gated fusion. In: *International Conference on Medical Image Computing and Computer-Assisted Intervention*. pp. 447–456. Springer (2019)
5. Dou, Q., de Castro, D.C., Kamnitsas, K., Glocker, B.: Domain generalization via model-agnostic learning of semantic features. In: *Advances in Neural Information Processing Systems*. pp. 6450–6461 (2019)
6. Ganin, Y., Ustinova, E., Ajakan, H., Germain, P., Larochelle, H., Laviolette, F., Marchand, M., Lempitsky, V.: Domain-adversarial training of neural networks. *The Journal of Machine Learning Research* **17**(1), 2096–2030 (2016)
7. Geirhos, R., Rubisch, P., Michaelis, C., Bethge, M., Wichmann, F.A., Brendel, W.: Imagenet-trained cnns are biased towards texture; increasing shape bias improves accuracy and robustness. In: *International Conference on Learning Representations* (2018)
8. Gonzalez, R.C., Woods, R.E., Eddins, S.L.: *Digital image processing using MATLAB*. Pearson Education India (2004)
9. Isensee, F., Jäger, P.F., Kohl, S.A., Petersen, J., Maier-Hein, K.H.: nnu-net: a self-configuring method for deep learning-based biomedical image segmentation. *Nature Methods* (2020)
10. Li, H., Zhang, J., Menze, B.: Generalisable cardiac structure segmentation via attentional and stacked image adaptation. *arXiv preprint arXiv:2008.01216* (2020)
11. Mach, F., Baigent, C., Catapano, A.L., Koskinas, K.C., Casula, M., Badimon, L., Chapman, M.J., De Backer, G.G., Delgado, V., Ference, B.A., et al.: 2019 esc/eas guidelines for the management of dyslipidaemias: lipid modification to reduce cardiovascular risk: The task force for the management of dyslipidaemias of the european society of cardiology (esc) and european atherosclerosis society (eas). *European Heart Journal* **41**(1), 111–188 (2020)
12. Tao, Q., Yan, W., Wang, Y., Paiman, E.H., Shamonin, D.P., Garg, P., Plein, S., Huang, L., Xia, L., Sramko, M., et al.: Deep learning-based method for fully automatic quantification of left ventricle function from cine mr images: a multivendor, multicenter study. *Radiology* **290**(1), 81–88 (2019)

13. Van der Walt, S., Schönberger, J.L., Nunez-Iglesias, J., Boulogne, F., Warner, J.D., Yager, N., Gouillart, E., Yu, T.: scikit-image: image processing in python. *PeerJ* **2**, e453 (2014)
14. Zhuang, X., Li, L.: Multi-sequence CMR based myocardial pathology segmentation challenge (Mar 2020). <https://doi.org/10.5281/zenodo.3715932>, <https://doi.org/10.5281/zenodo.3715932>